Experimental Study of Cucurbit[7]uril Derivatives Modified Acrylamide Polymer for Enhanced Oil Recovery

ARTICLE *in* INDUSTRIAL & ENGINEERING CHEMISTRY RESEARCH · APRIL 2014

Impact Factor: 2.59 · DOI: 10.1021/ie4037824

6 AUTHORS, INCLUDING:

Changjun Zou
Southwest Petroleum University
46 PUBLICATIONS **220** CITATIONS

SEE PROFILE

I&EC research
Industrial & Engineering Chemistry Research

Article

pubs.acs.org/IECR

Experimental Study of Cucurbit[7]uril Derivatives Modified Acrylamide Polymer for Enhanced Oil Recovery

Changjun Zou,*[,†] Tong Gu,[†] Pufu Xiao,[‡] Tingting Ge,[†] Meng Wang,[†] and Kai Wang[†]

[†]School of Chemistry and Chemical Engineering, Southwest Petroleum University, Chengdu 610500, People's Republic of China
[‡]Research Institute of Porous Flow and Fluid Mechanics, Chinese Academy of Sciences, Langfang 065007, People's Republic of China

Supporting Information

ABSTRACT: Acrylic acid cucurbit[7]uril ester (ACE) was prepared and utilized to react with acrylamide (AM) and hexadecyl dimethyl allyl ammonium chloride (C_{16}DMAAC) to synthesize a novel AM copolymer (AM/ACE/C_{16}DMAAC) through redox free-radical polymerization in aqueous solution. The chemical structure of AM/ACE/C_{16}DMAAC was confirmed by Fourier transform IR and ^{1}H NMR spectroscopies. Characterizations consisted of scanning electron microscopy, thermogravimetric analysis, and static light scattering, and the performance evaluations were conducted on several aspects such as intrinsic viscosity, stability, viscoelasticity, adsorption, and core-flooding experiments. Experiment results demonstrated the introduced ACE group could improve the salt tolerance and temperature resistance of polymer. Moreover, AM/ACE/C_{16}DMAAC could significantly increase the oil recovery of 21.43%. The superior performances of AM/ACE/C_{16}DMAAC revealed a potential application in high-temperature and high-mineralization oilfields for enhanced oil recovery.

1. INTRODUCTION

To maximize the exploitation of crude oil under permissions of economic and technical conditions, enhanced oil recovery (EOR) is the ultimate goal of oil reservoir exploitation. A large amount of residual oil is retained in the reservoir after water flooding. Because the water-soluble polymer can increase the viscosity of the displacing phase,[1,2] reduce the permeability of the aqueous phase, adjust the water/oil mobility ratio,[3−6] and achieve the purposes of expanding the volumetric sweep efficiency, polymer flooding has been used as an efficient technique for increasing the oil recovery in the tertiary recovery.[7]

Because of its good viscoelastic properties in the flooding process, polyacrylamide (PAM) has been widely used in oilfield chemical additives, thickeners, flocculants, surfactants, and so forth.[8−10] With the rapid development of oil exploitation techniques, the conventional acrylamide (AM) homopolymer cannot meet the requirements. In recent years, many researchers focused on preparing novel functionalized AM polymers to improve the temperature resistance, the salt tolerance, and the interactions with surfactants of the polymers.[11,12]

The supramolecular macrocyclic compound cucurbit[n]uril (CB[n]; n = 5, 6, 7, 8, 10) family is prepared through the condensation reaction of glycoluril and formaldehyde under acidic conditions.[13,14] All CB[n] compounds present a hydrophobic inner cavity that is accessible through two identical carbonyl-fringed portals.[15] The nonpolar inner cavity allows the hydrophobic or relatively hydrophobic guests of an appropriate size to form inclusion complexes, whereas the carbonyl-fringed portals allows electrostatic or ion−dipole interactions with positively charged functional groups of guest molecules. The rigid structure of CB[n] presents high thermal stability.[16] The special properties of the CB[n] compounds show an enormous potential in a variety of applications, including molecular recognition,[17−19] drug delivery,[20−23] self-assembly,[24,25] and catalytic reaction.[26] However, there was little report about the use of CB[n] to modify AM polymer for enhanced oil recovery due to its limited solubility in water.

In this work, we have sought to introduce the CB[7] group into synthesizing a novel hydrophobically associating AM polymer (AM/ACE/C_{16}DMAAC) to achieve the purpose of EOR in the tertiary stage. Acrylic acid cucurbit[7]uril ester (ACE) acts as the temperature-resistant and salt-tolerant monomer, while hexadecyl dimethyl allyl ammonium chloride (C_{16}DMAAC) acts as the hydrophobic monomer. A series of experiments is carried out to investigate the stability of AM/ACE/C_{16}DMAAC in high-temperature and high-mineralization conditions and its adsorption characterization while compared to PAM. In addition, the capacity of EOR is also evaluated.

2. EXPERIMENTAL SECTION

2.1. Materials. AM, C_{16}DMAAC, concentrated sulfuric acid, acetone, ammonium persulfate, sodium bisulfite, ethanol, sodium hydroxide, concentrated hydrochloric acid, and acrylic acid were analytical reagent grade. All of them were obtained from the Kelong Chemical Reagent Co., Ltd. (Chengdu, China). PerhydroxyCB[7] was prepared according to the method of Kim as described in the literature.[27] The viscosity-average molecular weight of PAM (Kelong, Chengdu) was 15 million, and the hydrolysis degree was 20%. The 80 mesh quartz sand was purchased from Jinjie Yuan Water Treatment Co., LTD (Chengdu, China). The apparent viscosity of the simulated crude oil from Bohai Oilfield was 154 mPa·s at 65 °C, and its API° was 21.9.

Received: November 8, 2013
Revised: March 29, 2014
Accepted: April 13, 2014
Published: April 23, 2014

dx.doi.org/10.1021/ie4037824 | Ind. Eng. Chem. Res. 2014, 53, 7570−7578

2.2. Synthesis of Monomer ACE. A 4.02 g amount of perhydroxyCB[7] was placed in a flask with a magnetic stirrer and dissolved in 60 mL of acrylic acid. Then, 1.84 g of concentrated sulfuric acid as a catalyst was added into the flask. The reaction mixture was heated to 90 °C for 6 h until producing a dark brown powder. After that, the resulting precipitate was filtered and washed by a large amount of acetone. The target product, a white powder, was obtained and dried under vacuum oven at 60 °C. The synthesized process is shown in Figure 1.

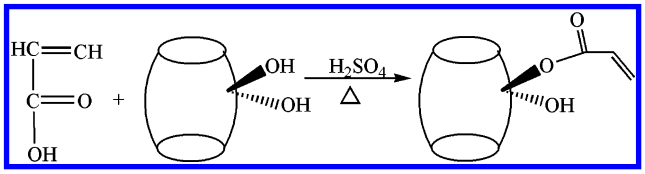

Figure 1. Synthesis of monomer ACE.

2.3. Synthesis of AM/ACE/C_{16}DMAAC and AM/C_{16}DMAAC. The monomers of AM/ACE/C_{16}DMAAC or AM/C_{16}DMAAC were dissolved in deionized water with a certain mass ratio, adjusting the pH of the solution to 7. Keeping the total monomers content of 20 wt %, the solution was further transferred into a three-necked flask placed in a thermostat water bath kettle. Then, the solution was purged with nitrogen for 30 min to remove oxygen at 25 °C. The initiator $(NH_4)_2S_2O_8$/$NaHSO_3$ (mass ratio = 2:1) whose concentration was 0.08 wt % relative to the total monomer feed was added when the temperature of the system reached 45 °C. Then, the mixture was kept stirring under nitrogen atmosphere until it turned to be viscous. Afterward, the reaction was continued for 4−5 h at 45 °C. Ultimately, a transparent gelatinous material was obtained after the mixture cooled to room temperature, which shall be washed repeatedly with ethanol until precipitating a white block solid. The solid was further dried under vacuum oven at 70 °C. The synthesized process is shown in Figure 2.

2.4. Characterization. Infrared spectra of AM/ACE/C_{16}DMAAC and ACE were obtained in the 400−4000 cm^{-1} region using a Nicolet Nexus 170SX Fourier transform infrared spectrophotometer on a KBr tablet. The spectra were acquired at a resolution of 4 cm^{-1}. The ^1H NMR spectra of AM/ACE/C_{16}DMAAC were recorded using a Bruker ASCEND-400 NMR spectrometer. $CDCl_3$ was used for field-frequency lock, and TMS was used for the internal standard. The surface morphologies of AM/ACE/C_{16}DMAAC, AM/C_{16}DMAAC, and PAM were observed by scanning electron microscopy (SEM; PHLIPS-XL30, Holland). The thermal properties of AM/ACE/C_{16}DMAAC and AM/C_{16}DMAAC were investigated by thermal gravimetric analysis (TGA), which was carried out on an STA 449F3 synchronal thermal analyzer (Germany) at a heating rate of 10 °C/min under air flow (60 mL/min) over a temperature range from room temperature up to 800 °C. The static light scattering measurements were performed on a BI-200SM light scattering detector at the wavelength of 532 nm. The refractive index increments of AM/ACE/C_{16}DMAAC in aqueous solutions were determined at 25 °C.

2.5. Intrinsic Viscosity of Copolymers. A NaCl solution of 1.0 mol/L was prepared as the solvent. The copolymer solution diluted with 2.0 mol/L NaCl solution was prepared as the sample solution (concentration of 0.001 g/mL copolymer, 1.00 mol/L NaCl). The Ubbelohde capillary viscometer was utilized to measure the relative and specific viscosities of polymer solutions at different concentrations. The viscosity-average molecular weights of AM/ACE/C_{16}DMAAC and AM/C_{16}DMAAC can be calculated from the intrinsic viscosity value by employing the Mark−Houwink equation.[28,29]

2.6. Stability Experiments. The properties of AM/ACE/C_{16}DMAAC were evaluated through stability experiments including salt tolerance, temperature resistance, and pH effect. Viscosity retention rate was an important indicator to evaluate the salt tolerance and temperature resistance of the polymer, which was calculated through the current viscosity divided by the initial viscosity. The effects of pH on polymer aqueous solutions of PAM and AM/ACE/C_{16}DMAAC were investigated at room temperature, and the pH was adjusted by 10 wt % HCl or 10 wt % NaOH aqueous solution. All of the viscosities were measured with a NDJ-8S viscometer. The measurement error was 5%, and the rotor speed was 60 rpm. The viscometer was adjusted by standard silicon oil at room temperature. The pH values were measured with a PHS-4C$^+$ acidity meter (Fangzhou, Chengdu). The concentrations of the corresponding polymer solutions in stability experiments were all 2000 mg/L.

2.7. Viscoelasticity of Polymers. Enhancing the viscoelasticity is beneficial to increasing the oil recovery.[30] The polymer with good viscoelasticity has a pulling effect to those small oil blocks in the dead angles of formation. So, it has an

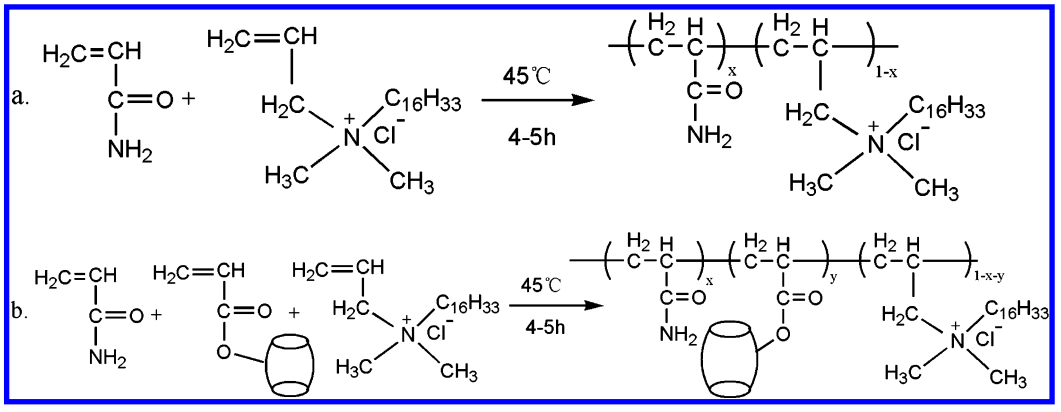

Figure 2. Synthesis of copolymers: (a) AM/C_{16}DMAAC, reaction conditions: AM:C_{16}DMAAC = 99.7:0.3, pH = 7.0, temperature = 45 °C, time = 4−5 h; (b) AM/ACE/C_{16}DMAAC, reaction conditions: AM:ACE:C_{16}DMAAC = 99.7:0.06:0.24, pH = 7.0, temperature = 45 °C, time = 4−5 h.

dx.doi.org/10.1021/ie4037824 | Ind. Eng. Chem. Res. 2014, 53, 7570−7578

obvious effect on improving the displacement efficiency of the polymer.

In this work, sinusoidal shear strain was applied on the polymer, while the stress was measured as a dynamic response. The elasticity modulus G' and viscous modulus G'' of solutions were mainly determined. AM/C_{16}DMAAC and AM/ACE/C_{16}DMAAC were scanned respectively in the oscillation frequency range of 0.1−10 s^{-1} at 25 °C. The concentrations of both polymer solutions were 2000 mg/L.

2.8. Static Adsorption Measurements. The 80−120 mesh quartz sand was selected as adsorbent, and the polymer solution was prepared with deionized water. Adsorption time was 48 h, and the solid−liquid ratio was 1:5 (g/mL). The static adsorption measurement was carried out at room temperature.

2.9. Core-Flooding Experiments. The experimental apparatus consisted of a constant speed pump (D-250L, made in Jiangsu Haian Oil Scientific Instruments Co., LTD in China), a multifunction core displacement device (YSF-1, made in Jiangsu Haian Oil Scientific Instruments Co., LTD in China), thermostat, pressure measuring system, intermediate container, and collecting container. Experiments were conducted by using the sand packs measuring 20 cm in length and 3.8 cm in diameter. The porosity of the sand pack was approximately 43.56%, and the water permeability was approximately 2.37 μm^2. The water phase for the core-flooding test was 2.0 wt % NaCl and 0.1 wt % $CaCl_2$. Five sets of experiments were conducted at 65 °C. All experiments were carried out in accordance with the following steps: First, filling the sand filling tube with quartz sand, and then, the saturated salt water was injected to measure the permeability and porosity. Second, injecting the simulated crude oil into the core until no water went out at the outlet. Third, the oil-bearing core was water flooded until the water cut reached 98%. Finally, a 0.3 PV polymer solution with the concentration of 2000 mg/L was injected into the core, and water flooding carried out again until the water cut reached 98%.[31]

3. RESULTS AND DISCUSSION

3.1. Characterizations of Copolymers. The chemical structures of ACE and AM/ACE/C_{16}DMAAC were confirmed by FT-IR spectroscopy as shown in Figure 3. From the spectrum curve of ACE, a strong absorption peak at 3432 cm^{-1} was attributed to the stretching vibration of −OH. The bands observed at 2956 and 2910 cm^{-1} were assigned to the stretching vibration peaks of $-CH_2-$. Furthermore, the peaks at 1729 and 1630 cm^{-1} were the characteristic absorption peaks of C═O and C═C, respectively, while the peak at 1115 cm^{-1} was attributed to the stretching vibration of C−O−C. It could be seen from Figure 3b that the absorption peak of the N−H stretching vibration presented at 3415 cm^{-1}. The characteristic absorptions of methyl and methylene groups were observed at 2925 and 2854 cm^{-1} respectively. These absorptions mentioned above demonstrated that the structure of ACE was presented in the copolymer. The absorptions of the C═O stretching vibration at 1677 cm^{-1} and the C−H bending vibration at 1454 cm^{-1} indicated the presence of a $-CONH_2$ group, which proved that the structure of AM was presented in the copolymer. The C═O group gave rise to a stronger absorption as it existed in both structures of ACE and AM. The absorption at 1317 cm^{-1} corresponded to the asymmetric stretching vibration of C−H, which was caused by the fact that a $-CH_3$ group connected with heteroatoms. The characteristic absorption at 1120 cm^{-1} was associated with the long-chain alkyl groups in C_{16}DMAAC. Therefore, a conclusion can be drawn from the FT-IR data that the target copolymer AM/ACE/C_{16}DMAAC was synthesized successfully.

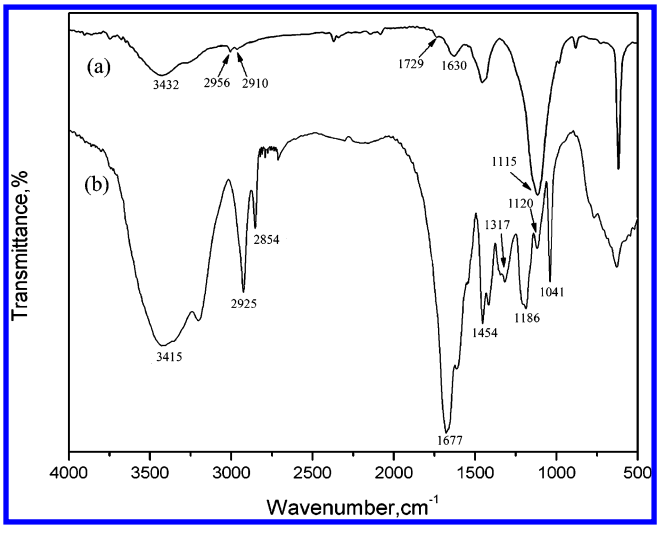

Figure 3. FT-IR spectra of (a) ACE and (b) AM/ACE/C_{16}DMAAC.

Figure 4 shows the ^{1}H NMR spectrum of AM/ACE/C_{16}DMAAC. The proton signals of −CH− (2.21 and 1.51 ppm) and $-CH_2-$ (2.05, 1.04 ppm) were associated with the main chain of the copolymer. The signal observed at 3.53 ppm contributed to the proton peak of $-CH_3$ bonded with the quaternary ammonium N^+. The proton peaks of $-CH_2-$ and $-CH_3$ in the long alkyl chain were 1.17 and 1.06 ppm, respectively. At 7.65 ppm, the proton peak of $-NH_2$ was monitored.[32] The data above indicated the existence of AM and C_{16}DMAAC. Furthermore, two sets of doublets around 5.60 and 4.20 ppm demonstrated the existence of CB[7] in ACE.[33] Thus, the data from the ^{1}H NMR spectrum was in accordance with that revealed by the FT-IR spectra.

Figure 5 shows the SEM images of AM/ACE/C_{16}DMAAC, AM/C_{16}DMAAC, and PAM. It was evident that the three polymers had typical gel-network structures. Compared to the structure of AM/C_{16}DMAAC, AM/ACE/C_{16}DMAAC had a more regular porous structure, and the size of the holes was more uniform and larger, whereas the network structure and holes of AM/C_{16}DMAAC appeared to be more disordered. In addition, the filamentous connections between molecular aggregates were much thicker than PAM and AM/C_{16}DMAAC.

The thermal gravimetric curves are shown in Figure 6. Combining the TGA data with DTG data, it could be found that both copolymers displayed four stages for the weight loss. The first stage was associated with the evaporation of intramolecular and intermolecular moisture, wherein AM/ACE/C_{16}DMAAC took place in the temperature range 40−216 °C with a mass loss of 6.32 wt %, while AM/C_{16}DMAAC took place in the range 40−214 °C with a mass loss of 7.01 wt %. The second stage of AM/ACE/C_{16}DMAAC occurred in the 216−336 °C temperature range with a mass loss of 15.90 wt %, while that of AM/C_{16}DMAAC took place in the 214−330 °C range with a mass loss of 16.65 wt %, which was due to the imine reaction of the amide groups and the decompositions of hydrophobic side chains. The third stage of AM/ACE/C_{16}DMAAC occurred in the 336−471 °C temperature range with a mass loss of 28.86 wt %, while that of AM/C_{16}DMAAC took place in the 330−441 °C range with a mass loss of 24.58

dx.doi.org/10.1021/ie4037824 | Ind. Eng. Chem. Res. 2014, 53, 7570−7578

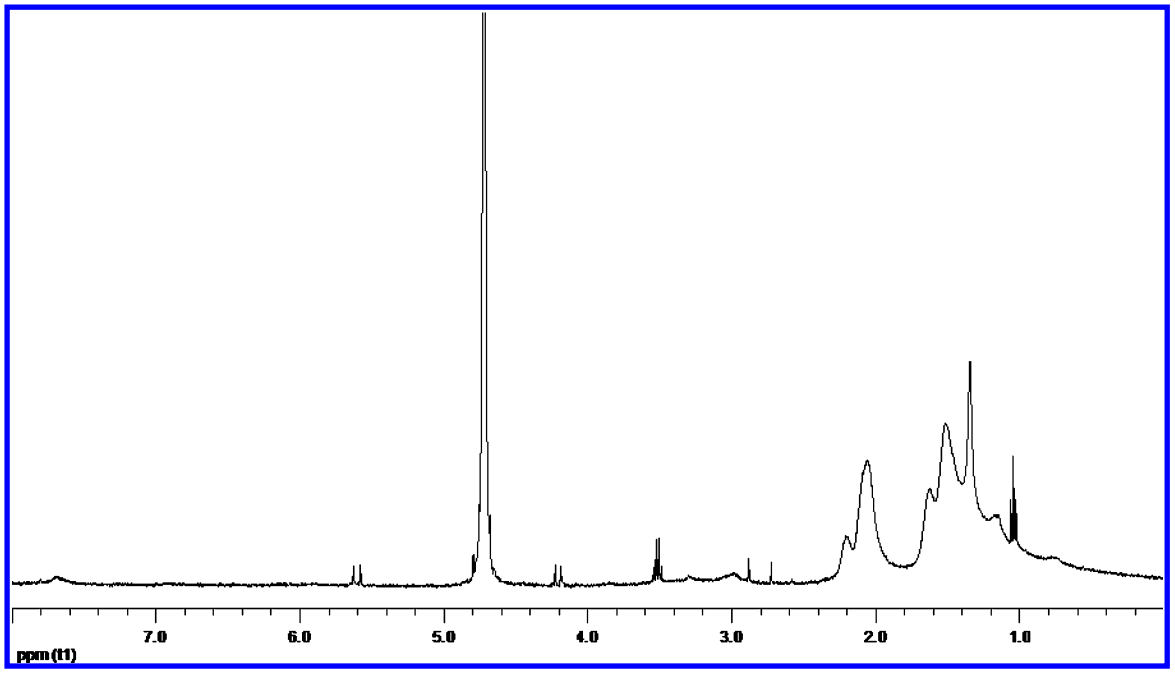

Figure 4. ^{1}H NMR spectra of AM/ACE/C_{16}DMAAC.

wt %, corresponding to the skeleton decompositions of the CB[7] occurring at around 450 °C. The final stage of AM/ACE/C_{16}DMAAC occurred beyond 471 °C with the mass loss of 38.56 wt %, while that of AM/C_{16}DMAAC occurred beyond 441 °C with the mass loss of 41.52 wt %, which was attributed to the carbonization. Moreover, comparing the DTG curves of both copolymers, it can be seen that the weight loss rate of AM/ACE/C_{16}DMAAC was slower than that of AM/C_{16}DMAAC before CB[7] has not been decomposed yet. The TG/DTG results indicated that the introduction of ACE can improve the thermal stability of copolymer.

3.2. Intrinsic Viscosity of Copolymers. The flow time of a 15 mL sample solution was measured and recorded as t_1; after that, the sample solution was diluted with adding 5, 5, 10, and 10 mL of solvent in four times, and its flow times were measured and recorded as t_2 to t_5, respectively. The flow time of the solvent was measured as t_0. All of the flow times were measured for three times and determined through the arithmetic mean value. By plotting the reduced viscosity (η_{sp}/C_r) or inherent viscosity ($\ln \eta_r/C_r$) against concentration (Figure 7), extrapolating to infinite dilution and taking the intercept, the intrinsic viscosities ($[\eta]$) of AM/ACE/C_{16}DMAAC and AM/C_{16}DMAAC were determined as 636.43 and 458.67 mL/g, respectively.

The viscosity-average molecular weight of the polymer can be calculated from $[\eta]$ through the Mark−Houwink equation, which AM/ACE/C_{16}DMAAC was 2.74×10^6 g/mol and AM/C_{16}DMAAC was 1.82×10^6 g/mol. It could be found that the intrinsic viscosity and molecular weight of AM/ACE/C_{16}DMAAC were larger than those of AM/C_{16}DMAAC. The reason could be related to the introduction of supermolecule CB[7]. Moreover, the hydrogen-bond interaction among ACE, AM, and C_{16}DMAAC made contributions to forming the supramolecular chain aggregates and network structure, and as a result, the viscosity of the copolymer solution further increased.

Figure 8 shows the static Zimm plot of AM/ACE/C_{16}DMAAC; extrapolating to infinite dilution and taking the intercept, the weight-average molar mass M_w was determined as 3.22×10^6 g/mol. Apparently, the value of M_w is more than that of $M\eta$, which is conform to the variation law of molecular weight of general polymers.

3.3. Viscosification Property of AM/ACE/C_{16}DMAAC. Aqueous solutions of AM/ACE/C_{16}DMAAC were prepared with different concentrations, and then, the apparent viscosities of each polymer solution were recorded at 50 °C. The relationship between polymer concentration and apparent viscosity is shown in Figure 9.

As shown in Figure 9, with the increase of the AM/ACE/C_{16}DMAAC concentration, the viscosity took a turning point at 1879 mg/L, which is called the critical association concentration C^*. When the concentration was below C^*, it generated an intramolecular hydrophobic microarea, and the molecular chains mainly existed in the form of curling configurations, which resulted in a decrease of hydrodynamic volume and a relatively lower viscosity. While the concentration was above C^*, it generated the intermolecular hydrophobic microarea, and meanwhile, the inclusion complex of CB[7] and the hydrophobic group formed. These resulted in the formation of supramolecular aggregates with the spatial network, so the viscosity increased sharply.

3.4. Salt-Tolerance Experiments. Salt solutions with a total salinity of 1.6×10^5 mg/L were prepared with NaCl, $CaCl_2$, and $MgCl_2$; it contained 2000 mg/L Ca^{2+} and 1000 mg/L Mg^{2+}, and the rest were Na^+ and Cl^-. Aqueous solutions of AM/ACE/C_{16}DMAAC, AM/C_{16}DMAAC, and PAM were prepared with deionized water, and salt solutions of the polymers were prepared subsequently. To evaluate the effect of different ACE contents on the salt tolerance, the apparent viscosities of the polymer solutions were determined at room temperature, and the viscosity retention rates were calculated. The experimental data are shown in Table 1, in which η_w was the apparent viscosity of the copolymer in aqueous solution and η_s was the apparent viscosity of the copolymer in salt solution.

As listed in Table 1, the viscosity of PAM reduced sharply in salt solution, and its retention rate was lower than that of AM/

dx.doi.org/10.1021/ie4037824 | Ind. Eng. Chem. Res. 2014, 53, 7570−7578

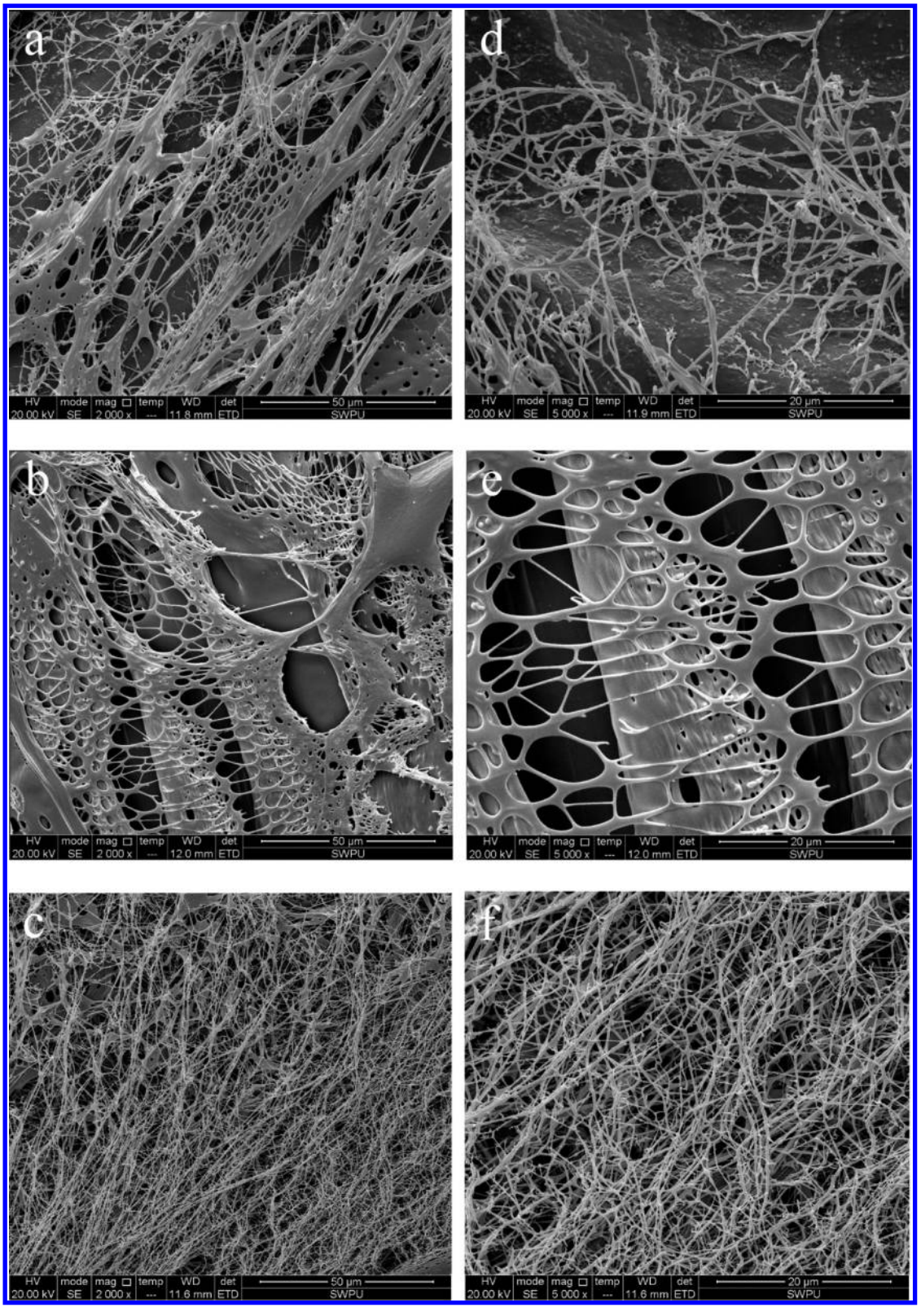

Figure 5. SEM images of copolymers: (a) AM/C_{16}DMAAC, magnified 2000 times; (b) AM/ACE/C_{16}DMAAC, magnified 2000 times; (c) PAM, magnified 2000 times; (d) AM/C_{16}DMAAC, magnified 5000 times; (e) AM/ACE/C_{16}DMAAC, magnified 5000 times; (f) PAM, magnified 5000 times.

C_{16}DMAAC and AM/ACE/C_{16}DMAAC, which was caused by the association between saline ions and the carboxyl group formed by the hydrolysis of PAM. This association caused the shrinkage of molecular chains, leading to a decline of viscosity. Moreover, it was found that the retention rates greatly increased with the rise of ACE content. Because the cavity of CB[7] preferred to form inclusion complex with positively charged salt ions in contrast with the cationic quaternary

dx.doi.org/10.1021/ie4037824 | *Ind. Eng. Chem. Res.* 2014, 53, 7570−7578

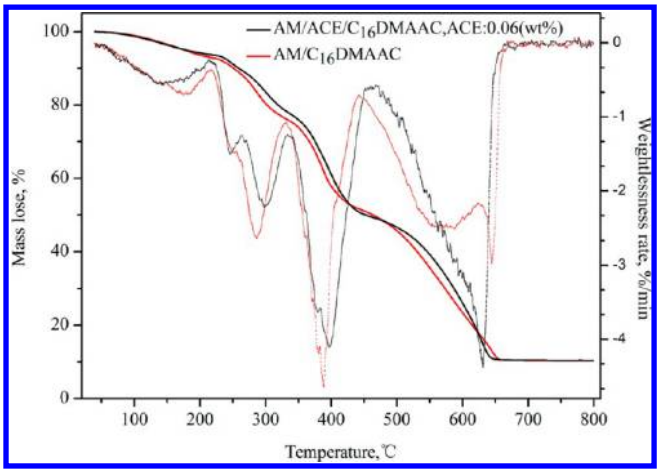

Figure 6. Thermal gravimetric curves of copolymers.

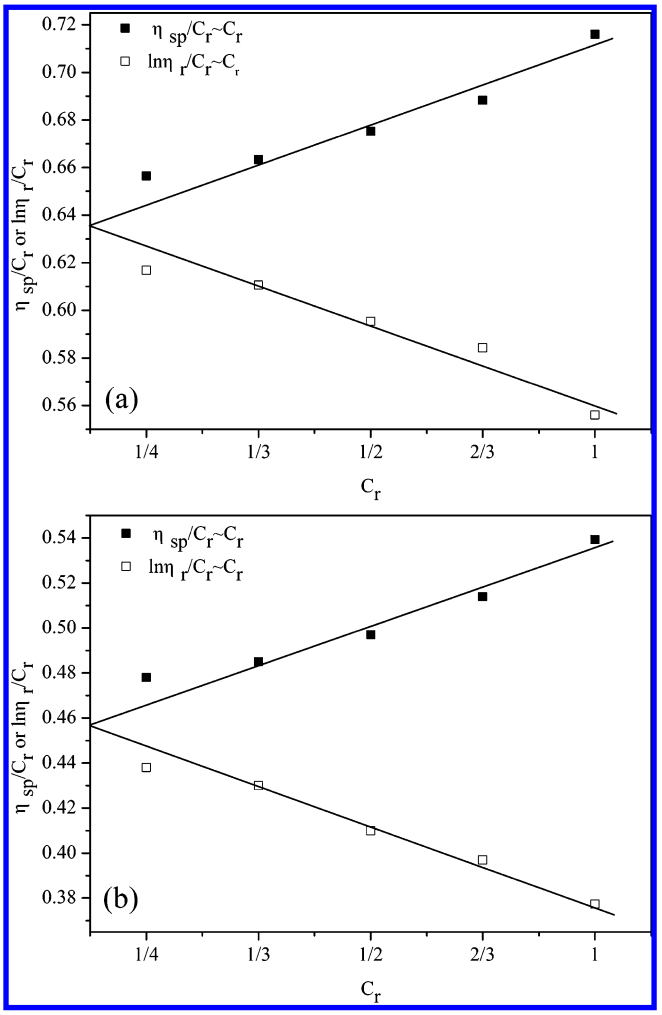

Figure 7. Relationship between η_{sp}/C_r (ln η_r/C_r) and C_r: (a) AM/ACE/C_{16}DMAAC; (b) AM/C_{16}DMAAC.

ammonium salt, the C_{16}DMAAC was more likely to be released from the inner cavity of CB[7]. With the presence of CB[7], the long hydrophobic chain became more stretch, and the molecular effective volume increased. Most important, CB[7] prevented saline ions from compressing the diffused double layer of AM effectively; thus, it weakened the effect of salt ions on the polymer to improve the salt tolerance. Therefore, the

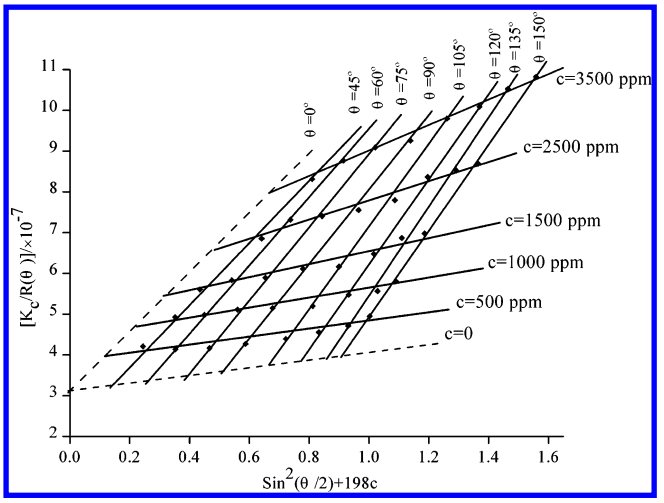

Figure 8. Zimm plot for AM/ACE/C_{16}DMAAC.

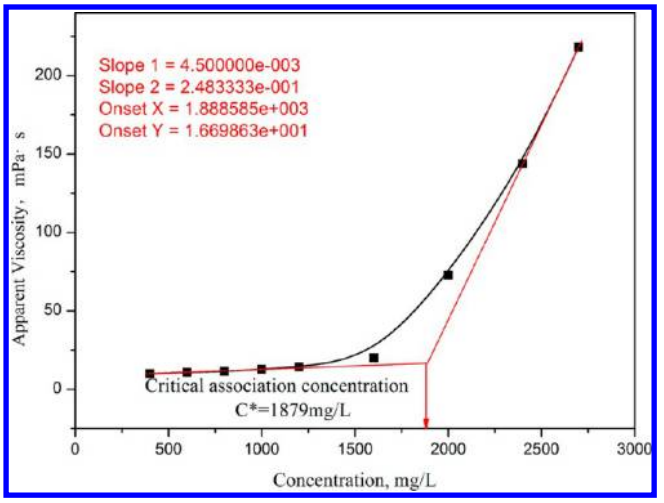

Figure 9. Relationship between apparent viscosity and concentration.

Table 1. Salt Tolerance of Copolymers

entry	polymer	ACE contents (wt %)	η_w (mPa/s)	η_s (mPa/s)	retention rate (%)
1	PAM	–	84.3	13.4	15.90
2	AM/ C_{16}DMAAC	–	34.5	14.3	41.44
3	AM/ACE/ C_{16}DMAAC	0.06	82.0	73.3	89.39
4	AM/ACE/ C_{16}DMAAC	0.075	76.3	70.7	92.66
5	AM/ACE/ C_{16}DMAAC	0.15	58.8	54.9	93.36

addition of ACE enhanced the salt tolerance of AM/ACE/C_{16}DMAAC. Combining with the viscosity data, the salt tolerance of AM/ACE/C_{16}DMAAC would be even better when controlling the introduced ACE amount at around 0.06 wt %.

3.5. Temperature-Resistance Experiments. The effects of ACE content on viscosities of the copolymer solutions at different temperatures have been investigated, wherein the concentration of the polymer solution was 2000 mg/L and the total salinity was 1.6×10^5 mg/L. The apparent viscosities of the polymers were determined with a digital viscometer at 25, 45, 65, and 85 °C, and the results were illustrated in Figure 10.

dx.doi.org/10.1021/ie4037824 | Ind. Eng. Chem. Res. 2014, 53, 7570−7578

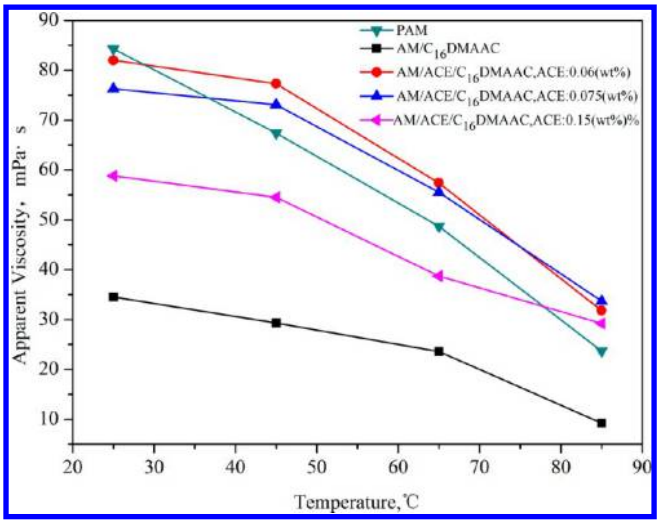

Figure 10. Temperature resistance of copolymers.

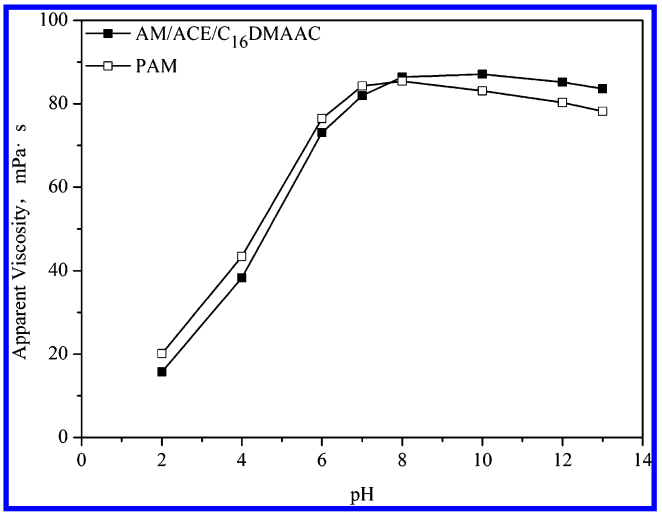

Figure 11. Effect of pH on the polymer solutions.

As shown from the curves, for all polymer solutions, the apparent viscosity decreased with the increase of the temperature. As the temperature increased, the intermolecular thermal motion rate sped up, causing the molecular energy to be greater than the intermolecular association in the copolymer and resulting in the dissociation of the supramolecular system and a reduction of apparent viscosity. The carbonyl-fringed portals of CB[7] allows electrostatic interactions with a positively charged branched chain; thus, the increased ACE content would make a reduction of molecular volume and resulted in the decrease of initial viscosity. Moreover, when the temperature was at 85 °C, the viscosity retention rates of PAM and AM/C_{16}DMAAC were 28.1% and 26.6%, respectively, while the retention rates of AM/ACE/C_{16}DMAAC contained with 0.06, 0.075, and 0.15 wt % ACE were 38.78%, 44.16%, and 49.65%, respectively. It was found that the decreasing speed of the viscosity varied with the introduced ACE dosage and an increase in the viscosity retention rate was obtained with increasing the content of ACE in the copolymer. This proved that the addition of ACE improved the temperature resistance of the copolymer and the copolymer could maintain a relatively higher viscosity than PAM even at a high temperature of 85 °C.

3.6. pH Tests. The comparison of the pH effect on the polymer solutions is shown in Figure 11. As seen from the curves, the viscosities of AM/ACE/C_{16}DMAAC and PAM first increased rapidly at the pH range 2−6 then increased slowly when the pH increased from 7 to 8. Afterward, the viscosity of PAM slowly decreased with the further increase of pH. In contrast, the viscosity of AM/ACE/C_{16}DMAAC continued to increase slowly until the pH value exceeded 10. The reason could be explained as follows. With the increase of pH, amide groups began to take the hydrolysis leading to an increase of viscosity. When the pH increased to a certain extent, the viscosity of PAM slowly decreased due to the presence of Na^+ ions. Since the cavity of CB[7] had an inclusion effect with a certain number of Na^+ ions, the reduction of the viscosity of AM/ACE/C_{16}DMAAC occurred at a higher pH value than that of PAM, and the viscosity downtrend of AM/ACE/C_{16}DMAAC was smaller.

3.7. Viscoelasticity Experiments. The comparison of elasticity modulus and viscous modulus among copolymers were investigated, and the results are shown in Figure 12. The elasticity modulus G' and viscous modulus G'' reflected the

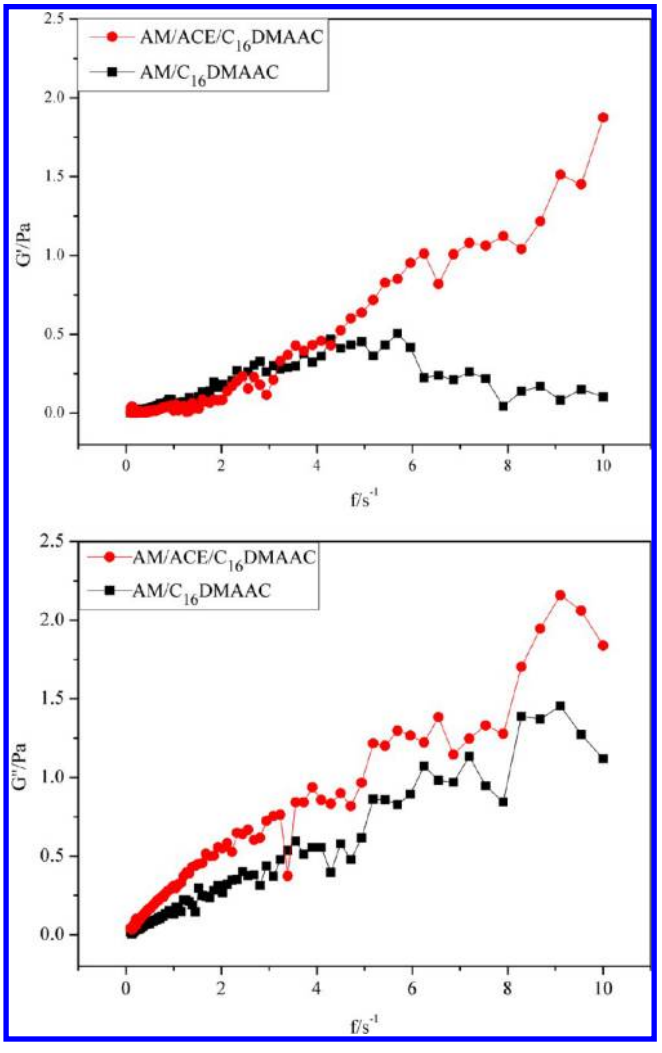

Figure 12. Viscoelasticity of AM/ACE/C_{16}DMAAC and AM/C_{16}DMAAC: (a) elasticity modulus G'; (b) viscous modulus G''.

elasticity and viscosity of the solution, respectively. As seen from Figure 12a, both polymers showed low elasticity in the low-frequency region. However, with the increase of frequency, the elasticity modulus of AM/ACE/C_{16}DMAAC increased, while that of AM/C_{16}DMAAC slightly decreased. As shown in

dx.doi.org/10.1021/ie4037824 | Ind. Eng. Chem. Res. 2014, 53, 7570−7578

Figure 12b, the high frequency would lead to an increase of the viscous modulus of both polymers. However, the viscosity of AM/ACE/C_{16}DMAAC was higher than AM/C_{16}DMAAC either in the low-frequency region or the high-frequency region. The reasons for AM/ACE/C_{16}DMAAC performing with better viscoelasticity than AM/C_{16}DMAAC could be explained as follows. The viscoelasticity of AM/C_{16}DMAAC was caused by the entanglement between molecular chains, while that of AM/ACE/C_{16}DMAAC was contributed to the hydrophobic association between the molecular chains in addition to the entanglement. The loss angle tangents of the both copolymers were greater than 1, which means both of the copolymer solutions gave priority to exhibit the viscous characteristics.

3.8. Static Adsorption Measurements. The adsorption curves of PAM and AM/ACE/C_{16}DMAAC are shown in Figure 13. It could be found that, when the concentration was less

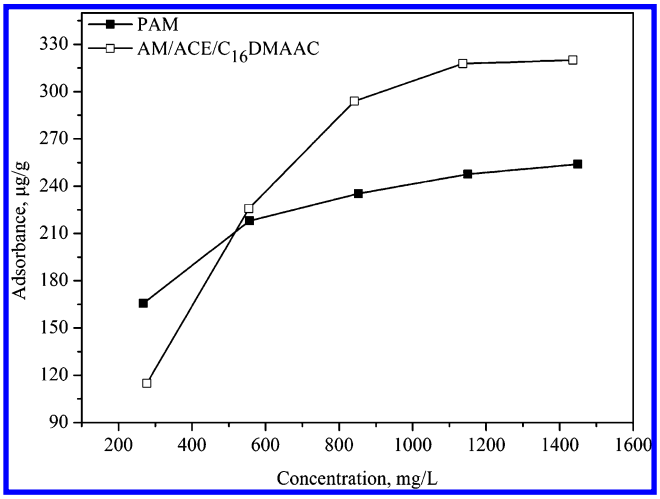

Figure 13. Adsorption isotherms of PAM and AM/ACE/C_{16}DMAAC.

than 518 mg/L, the adsorbance of PAM was larger than that of AM/ACE/C_{16}DMAAC and when the concentration exceeded 518 mg/L the trend reversed. The maximum adsorbance of PAM was 254 μg/g, while that of AM/ACE/C_{16}DMAAC was 320 μg/g. At the stage of low concentration (<518 mg/L), the hydrophobic group of AM/ACE/C_{16}DMAAC mainly formed an intramolecular association. Meanwhile, polymers on the quartz sand surface gave priority to form monolayer adsorption. On the other hand, the molecular weight of AM/ACE/C_{16}DMAAC was smaller than that of PAM. These resulted in a larger adsorbance of PAM. With the increase of polymer concentration, the hydrophobic group of AM/ACE/C_{16}DMAAC mainly formed an intermolecular association. At the moment, AM/ACE/C_{16}DMAAC was adsorbed on the quartz sand surface by the hydrophobic association. The adsorption behavior of the polymers gave priority to form multilayer adsorption. Thus, the adsorbance of AM/ACE/C_{16}DMAAC turned larger than that of PAM.

3.9. Core-Flooding Experiments. The concentrations of the polymer solutions were 2000 mg/L. In all core-flooding tests, when the polymer solution was injected, the pressure value was controlled less than 0.18 MPa. The results of the core-flooding experiments are shown in Table 2.

The core-flooding experiment results demonstrated that both AM/C_{16}DMAAC and AM/ACE/C_{16}DMAAC were able to increase residual oil recovery, and their flooding capacities were

Table 2. Results of the Core-Flooding Experiments

sample	polymer	ACE contents (wt %)	E_1[a] (%)	E_2[b] (%)	EOR[c] (%)
1	PAM	–	46.13	53.04	6.91
2	AM/C_{16}DMAAC	–	43.93	53.16	9.23
3	AM/ACE/C_{16}DMAAC	0.06	46.07	67.50	21.43
4	AM/ACE/C_{16}DMAAC	0.075	44.31	55.43	11.12
5	AM/ACE/C_{16}DMAAC	0.15	42.83	53.17	10.34

[a]E_1 is the oil recovery ratio by water flooding. [b]E_2 is the total oil recovery ratio. [c]EOR is determined by E_2 minus E_1.

better than that of PAM. The EOR of sample no. 3 can reach a value of 21.43% might be due to its relatively higher viscosity than other samples. From the perspective of the polymer itself, since the introduction of CB[7] and C_{16}DMAAC increased the molecular weight of the polymer and the hydrophobic long chain of the polymer produced the hydrophobic association effects, sample no. 3 owned a better viscoelasticity. All of these were conductive to displace those small oil blocks in the dead angles effectively.

4. CONCLUSIONS

The novel cucurbit[7]uril derivative modified AM polymer AM/ACE/C_{16}DMAAC was synthesized by aqueous free-radical polymerization, and its chemical structure was confirmed by FT-IR and ^{1}H NMR spectroscopies. Furthermore, the microstructures of the copolymers were compared by SEM. Performance experiments including intrinsic viscosity, stability, viscoelasticity, adsorption, and core-flooding tests were carried out to evaluate the properties of AM/ACE/C_{16}DMAAC. Experimental results demonstrated that AM/ACE/C_{16}DMAAC possessed a typical network structure and the introduced ACE group could enhance the viscoelastic property, temperature resistance, and salt tolerance. AM/ACE/C_{16}DMAAC, which consisted of 99.7 wt % AM, 0.06 wt % ACE, and 0.24 wt % C_{16}DMAAC, could enhance the oil recovery of 21.43%. These excellent aspects indicated that AM/ACE/C_{16}DMAAC has a potential application in high-temperature and high-mineralization oilfields for EOR.

■ ASSOCIATED CONTENT

Supporting Information

Thermal stabilities of AM/ACE/C_{16}DMAAC and PAM; and figure of single tube flooding test of AM/ACE/C_{16}DMAAC (sample no. 3). This material is available free of charge via the Internet at http://pubs.acs.org.

■ AUTHOR INFORMATION

Corresponding Author

*Tel.: +86 02883037327. Fax: +86 02883037305. E-mail: changjunzou@126.com.

Notes

The authors declare no competing financial interest.

■ ACKNOWLEDGMENTS

This work was financial supported by National Natural Science Foundation of China, China National Petroleum Corporation Petrochemical Unite Funded Project (U1262111).

REFERENCES

(1) Needham, R. B.; Doe, P. H. Polymer flooding review. *J. Pet. Technol.* **1987**, *39*, 1503−1507.

(2) Kaminsky, R. D.; Wattenbarger, R. C.; Szafranski, R. C.; Coutee, A. S. Guidelines for polymer flooding evaluation and development. Presented at the International Petroleum Technology Conference, Dubai, U.A.E., Dec 4−6, 2007; paper SPE 11200.

(3) Sabhapondit, A.; Borthakur, A.; Haque, I. Water soluble acrylamidomethyl propane sulfonate (AMPS) copolymer as an enhanced oil recovery chemical. *Energy Fuels* **2003**, *17*, 683−688.

(4) Chang, H. L. Polymer flooding technology-yesterday, today, and tomorrow. *J. Pet. Technol.* **1978**, *30*, 1113−1128.

(5) Gogarty, W. B. Micellar/polymer flooding an overview. *J. Pet. Technol.* **1978**, *30*, 1089−1101.

(6) Yao, C.; Lei, G.; Li, L.; Gao, X. Selectivity of pore-scale elastic microspheres as a novel profile control and oil displacement agent. *Energy Fuels* **2012**, *26*, 5092−5101.

(7) Bai, Y.; Li, J.; Zhou, J.; Li, Q. Sensitivity analysis of the dimensionless parameters in scaling a polymer flooding reservoir. *Transp. Porous Media* **2008**, *73*, 21−37.

(8) Guo, Y. J.; Liu, J. X.; Guo, Y. J.; Zhang, X. M.; Feng, R. S.; Li, H. B.; Zhang, J.; Lv, X.; Luo, P. Y. Displacement characters of combination flooding systems consisting of gemini-nonionic mixed surfactant and hydrophobically associating polyacrylamide for Bohai OffshoreOilfield. *Energy Fuels* **2012**, *26*, 2858−2864.

(9) Rabiee, A.; Zeynali, M. E.; Baharvand, H. Synthesis of high molecular weight partially hydrolyzed polyacrylamide and investigation on its properties. *Iran. Polym. J.* **2005**, *14*, 603−608.

(10) Farajzadeh, R.; Ameri, A.; Faber, M. J.; van Batenburg, D. W.; Boersma, D. M.; Bruining, J. Effect of continuous, trapped, and flowing gas on performance of alkaline surfactant polymer (ASP) flooding. *Ind. Eng. Chem. Res.* **2013**, *52*, 13839−13848.

(11) Ponnapati, R.; Karazincir, O.; Dao, E.; Ng, R.; Mohanty, K. K.; Krishnamoorti, R. Polymer-functionalized nanoparticles for improving waterflood sweep efficiency: Characterization and transport properties. *Ind. Eng. Chem. Res.* **2011**, *50*, 13030−13036.

(12) Zhao, Q.; Sun, J.; Lin, Y.; Zhou, Q. Study of the properties of hydrolyzed polyacrylamide hydrogels with various pore structures and rapid pH-sensitivities. *React. Funct. Polym.* **2010**, *70*, 602−609.

(13) Freeman, W. A.; Mock, W. L.; Shih, N. Y. Cucurbituril. *J. Am. Chem. Soc.* **1981**, *103*, 7367−7368.

(14) Kim, J.; Jung, I. S.; Kim, S. Y.; Lee, E.; Kang, J. K.; Sakamoto, S.; Yamaguchi, K.; Kim, K. New cucurbituril homologues: Syntheses, isolation, characterization, and X-ray crystal structures of cucurbit[*n*]-uril (*n* = 5, 7, and 8). *J. Am. Chem. Soc.* **2000**, *122*, 540−541.

(15) Nau, W. M.; Florea, M.; Assaf, K. I. Deep inside cucurbiturils: Physical properties and volumes of their inner cavity determine the hydrophobic driving force for host−guest complexation. *Isr. J. Chem.* **2011**, *51*, 559−577.

(16) Lagona, J.; Mukhopadhyay, P.; Chakrabarti, S.; Isaacs, L. The cucurbit[n]uril family. *Angew. Chem., Int. Ed.* **2005**, *44*, 4844−4870.

(17) Gamal-Eldin, M. A.; Macartney, D. H. Selective molecular recognition of methylated lysines and arginines by cucurbit[6]uril and cucurbit[7]uril in aqueous solution. *Org. Biomol. Chem.* **2013**, *11*, 488−495.

(18) Yi, S.; Captain, B.; Ottaviani, M. F.; Kaifer, A. E. Controlling the extent of spin exchange coupling in 2,2,6,6-tetramethylpiperidine-1-oxyl (TEMPO) biradicals via molecular recognition with cucurbit[*n*]-uril hosts. *Langmuir* **2011**, *27*, 5624−5632.

(19) Urbach, A. R.; Ramalingam, V. Molecular recognition of amino acids, peptides, and proteins by cucurbit[*n*]uril receptors. *Isr. J. Chem.* **2011**, *51*, 664−678.

(20) Walker, S.; Kaur, R.; Mcinnes, F. J.; Wheate, N. J. Synthesis, processing and solid state excipient interactions of cucurbit[6]uril and its formulation into tablets for oral drug delivery. *Mol. Pharmaceutics* **2010**, *7*, 2166−2172.

(21) Saleh, N. I.; Meetani, M. A.; Al-Kaabi, L.; Ghosh, I.; Nau, W. M. Effect of cucurbit[*n*]urils on tropicamide and potential application in ocular drug delivery. *Supramol. Chem.* **2011**, *23*, 650−656.

(22) Kenndy, A. R.; Florence, A. J.; Mclnnes, F. J.; Wheate, N. J. A chemical preformulation study of a host−guest complex of cucurbit[7]uril and a multinuclear platinum agent for enhanced anticancer drug delivery. *Dalton Trans.* **2009**, *37*, 7695−7700.

(23) Wheate, N. J. Improving platinum(II)-based anticancer drug delivery using cucurbit[n]urils. *J. Inorg. Biochem.* **2008**, *102*, 2060−2066.

(24) Vinciguerra, B.; Cao, L.; Cannon, J. R.; Zavalij, P. Y.; Fenselau, C.; Isaacs, L. Synthesis and self-assembly processes of monofunctionalized cucurbit[7]uril. *J. Am. Chem. Soc.* **2012**, *134*, 13133−13140.

(25) Li, J.; Zhou, L.; Luo, Q.; Wang, Y.; Zhang, C.; Lu, W.; Xu, J.; Liu, J. Cucurbit[7]uril-based vesicles formed by self-assembly of supramolecular amphiphiles. *Chin. J. Chem.* **2012**, *30*, 2085−2090.

(26) Basilio, N.; Garcia-Rio, L.; Moreira, J. A.; Pessego, M. Supramolecular catalysis by cucurbit[7]uril and cyclodextrins: Similarity and differences. *J. Org. Chem.* **2010**, *75*, 848−855.

(27) Jon, S. Y.; Selvapalam, N.; Oh, D. H.; Kang, J. K.; Kim, S. Y.; Jeon, Y. J.; Lee, J. W.; Kim, K. Facile synthesis of cucurbit[*n*]uril derivatives via direct functionalization: Expanding utilization of cucurbit[*n*]uril. *J. Am. Chem. Soc.* **2003**, *125*, 10186−10187.

(28) Zeynali, M. E.; Rabii, A.; Baharvand, H. Synthesis of partially hydrolyzed polyacrylamide and investigation of solution properties (viscosity behaviour). *Iran. Polym. J.* **2004**, *13*, 479−484.

(29) Zou, C.; Zhao, P.; Hu, X.; Yan, X.; Zhang, Y.; Wang, X.; Song, P.; Luo, P. *β*-Cyclodextrin-functionalized hydrophobically associating acrylamide copolymer for enhanced oil recovery. *Energy Fuels* **2013**, *27*, 2827−2834.

(30) Veerabhadrappa, S. K.; Trivedi, J. J.; Kuru, E. Visual confirmation of the elasticity dependence of unstable secondary polymer floods. *Ind. Eng. Chem. Res.* **2013**, *52*, 6234−6241.

(31) Hou, J.; Liu, Z.; Zhang, S.; Yue, X.; Yang, J. The role of viscoelasticity of alkali/surfactant/polymer solutions in enhanced oil recovery. *J. Pet. Sci. Eng.* **2005**, *47*, 219−235.

(32) Yang, Z. L.; Gao, B. Y.; Li, C. X.; Yue, Q. Y.; Liu, B. Synthesis and characterization of hydrophobically associating cationic polyacrylamide. *Chem. Eng. J.* **2010**, *161*, 27−33.

(33) Saleh, N.; Khaleel, A.; Al-Dmour, H.; Al-Hindawi, B.; Yakushenko. Host−guest complexes of cucurbit [7] uril with albendazole in solid state. *J. Therm. Anal. Calorim.* **2013**, *111*, 385−392.